Geophysical Research Letters

RESEARCH LETTER
10.1029/2018GL081175

Key Points:
- The observed Arabian Sea warming changes (slowdown and acceleration) are linked to the Atlantic multidecadal oscillation for the first time
- The teleconnection involves air-sea interactions across multiple ocean basins, with a contribution from western Pacific that acts as a relay
- The decadal phase shift of Atlantic-Western Pacific trans-basin variability since the 1990s contributes to the rapid warming of Arabian Sea

Supporting Information:
- Supporting Information S1

Correspondence to:
C. Sun,
scheng@bnu.edu.cn

Citation:
Sun, C., Li, J., Kucharski, F., Kang, I.-S., Jin, F.-F., Wang, K., et al. (2019). Recent acceleration of Arabian Sea warming induced by the Atlantic-western Pacific trans-basin multidecadal variability. *Geophysical Research Letters*, *46*, 1662–1671. https://doi.org/10.1029/2018GL081175

Received 2 NOV 2018
Accepted 18 JAN 2019
Accepted article online 28 JAN 2019
Published online 8 FEB 2019

Recent Acceleration of Arabian Sea Warming Induced by the Atlantic-Western Pacific Trans-basin Multidecadal Variability

Cheng Sun[1], Jianping Li[1,2], Fred Kucharski[3,4], In-Sik Kang[5], Fei-Fei Jin[6], Kaicun Wang[1], Chunzai Wang[7], Ruiqiang Ding[8], and Fei Xie[1]

[1]College of Global Change and Earth System Science (GCESS), Beijing Normal University, Beijing, China, [2]Laboratory for Regional Oceanography and Numerical Modeling, Qingdao National Laboratory for Marine Science and Technology, Qingdao, China, [3]The Abdus Salam International Centre for Theoretical Physics, Trieste, Italy, [4]Center of Excellence for Climate Change Research/Department of Meteorology, King Abdulaziz University, Jeddah, Saudi Arabia, [5]Indian Ocean Operational Oceanographic Research Center, SOED/Second Institute of Oceanography, Hangzhou, China, [6]Department of Atmospheric Sciences, SOEST, University of Hawai'i at Mānoa, Honolulu, HI, USA, [7]State Key Laboratory of Tropical Oceanography (LTO), South China Sea Institute of Oceanology, Chinese Academy of Sciences, Guangzhou, China, [8]State Key Laboratory of Numerical Modeling for Atmospheric Sciences and Geophysical Fluid Dynamics, Institute of Atmospheric Physics, Chinese Academy of Sciences, Beijing, China

Abstract Arabian Sea (AS) warming has been significantly accelerated since the 1990s, in particular in the spring season. Here we link the AS warming changes to the Atlantic multidecadal oscillation (AMO). A set of Atlantic pacemaker experiments with a slab mixed-layer ocean model successfully reproduces the AS spring multidecadal variability and its connection with the AMO. An atmospheric teleconnection from the Atlantic to the AS in the preceding winter and associated thermodynamic air-sea feedback is found to be important. The teleconnection can be reestablished by the atmospheric model when the AMO sea surface temperature (SST) and its trans-basin footprint over the western Pacific are prescribed simultaneously. The western Pacific SST warming associated with the AMO positive phase induces a Gill-type Rossby wave over the AS, showing anomalously low pressures and converging southerlies that weaken winter northerlies. Thus, the wind-evaporation-SST feedback results in and maintains the AS warm SST anomalies to the subsequent spring.

Plain Language Summary The rapid warming of the Arabian Sea (AS) since the 1990s not only has significant impacts on the monsoon climate change and extreme weather events (flood, heat wave, and cyclone) in Arabian Peninsula and Indian subcontinent but also poses increasingly severe risks of damage to the coastal and marine ecosystems. However, the cause of this recent acceleration of AS warming remains unclear. Here using observations and atmosphere-ocean coupled models, we link the observed AS warming changes to the Atlantic multidecadal oscillation (AMO) and show that more than 70% of AS multidecadal variability can be explained by the AMO. This Atlantic-AS teleconnection involves atmosphere-ocean interactions across multiple ocean basins, with a contribution from the western Pacific (WP). The SST footprint of the AMO over the WP acts as a relay for the effect of the AMO on the AS by exciting an atmospheric teleconnection and subsequently thermodynamic feedbacks over the AS. The concurrent cold-to-warm phase shift of the AMO and its WP SST footprint since the 1990s contribute constructively to the rapid warming of the AS. Our results highlight an unexpected multiple-basin interaction at decadal timescales, which plays a key role in the attribution of historical regional SST warming.

1. Introduction

Observations show that all major ocean basins around the world have been warming up since the beginning of the twentieth century, and this century-scale warming trend has been linked to the global effect of anthropogenic greenhouse gas emissions (Trenberth et al., 2007). Even so, the warming rates of sea surface temperature (SST) over the three basins are different, possibly due to the modulation of internal decadal SST variability (Lovsletten & Rypdal, 2016; Swanson et al., 2009). In the Pacific and Atlantic basins, there are two major modes of internal decadal climate variability: Interdecadal Pacific Oscillation (IPO; Parker et al., 2007) and Atlantic Multidecadal Oscillation (AMO; Enfield et al., 2001;

Knight et al., 2005; Sun et al., 2015). In addition, there arises a strong trans-basin SST teleconnection from the North Atlantic to the Pacific on multidecadal timescales (Kucharski et al., 2015; Zhang & Delworth, 2007), leading to significant SST footprints of the AMO over the Pacific basin, such as the western Pacific (Sun et al., 2017).

The secular SST warming trend of the Indian Ocean is stronger than most of the tropical Pacific and Atlantic, especially since the 1950s (Du & Xie, 2008; Han, Vialard, et al., 2014; Roxy et al., 2014; Roxy et al., 2015), but the observed multidecadal SST variability over the Indian Ocean is much weaker than the Pacific and Atlantic Oceans. In spite of this, existing studies have suggested a remote influence of IPO (Pacific decadal oscillation in some studies) on multidecadal variability of Indian Ocean Basin mode (Deser et al., 2004; Dong et al., 2016; Han, Meehl, et al., 2014), which is a leading mode of Indian Ocean SST variability and characterized by a basin-wide uniform structure (Schott et al., 2009). However, this Pacific-Indian Ocean relationship is nonstationary and has broken down since the 1980s (Dong & Mcphaden, 2017b), suggesting that other mechanisms need to be taken into consideration for the Indian Ocean multidecadal variability. On the other hand, the role of the Atlantic Ocean in influencing the Indian Ocean on multidecadal timescales is much less understood.

Besides the coherent SST change associated with the Indian Ocean Basin mode, SST variability over the Indian Ocean also exhibits regional features. As a part of the Indian Ocean, the Arabian Sea (AS) has received a lot of attention due to its geographical location and its important impacts on the surrounding regions (Shukla & Misra, 1977). There is strong interaction between the upper ocean of the AS and the Asia monsoon (Izumo et al., 2008; Li et al., 2001; Schott et al., 2009; Vecchi et al., 2004; Vinayachandran, 2004).

A secular warming trend of AS SST is observed throughout the twentieth century (Dinesh Kumar et al., 2016; Kumar et al., 2009). However, the multidecadal warming rate (amount of warming over decades) of AS SST is not constant but varies in time. The rate of SST increase for the period 1960–2009 reaches 0.12 °C per decade, much stronger than the previous period of 1900–1950 (0.008 °C per decade; Dinesh Kumar et al., 2016; D'Mello & Prasanna Kumar, 2018). Furthermore, the warming rate has been reported to be accelerated since the early 1990s, and this causes a climate regime shift (D'Mello & Prasanna Kumar, 2018; Kumar et al., 2009). This rapid warming brings an increased risk of extreme weather and climate events, such as floods (Roxy et al., 2017), heat waves (Trenberth & Fasullo, 2012), and cyclones (Murakami et al., 2017). However, the mechanism responsible for the recent acceleration of AS warming remains elusive.

This study combines the analysis of observations and atmosphere-ocean coupled model simulations to explore the physical mechanism for the recent acceleration of AS SST warming. The seasonality and spatial characteristics associated with the warming acceleration are identified, and multidecadal variability of AS SST is discussed in context of its modulation of the warming rate. The remote influence from multidecadal variability of other basins (i.e., the AMO and Atlantic-western Pacific trans-basin multidecadal variability) and the physical mechanism are further investigated.

2. Data and Methodology

2.1. Data Sets

Three data sets of the global observational SST are used in this study including the Kaplan SST data set (Kaplan et al., 1998), the Hadley Centre SST (HadSST3) data set (Kennedy et al., 2011), and the extended reconstruction SST version 3 (ERSST v3b) data set (Smith et al., 2008). Uncertainties in global SST observations prior to 1900 are large, and the data before 1900 are less reliable (Folland et al., 2001). Therefore, the analysis of global SST variability is confined to the post-1900 period for the SST data sets.

The Twentieth Century Reanalysis version 2 (20CR2) was used to analyze the sea level pressure, surface winds, and sea surface heat flux in the present study, and all heat fluxes are defined positive downward. The 20CR2 reanalysis is produced by assimilating surface pressure observations along with a prescribed SST boundary condition. However, due to the low observation density in the first half of the twentieth century and a drop of the global number of assimilated observations before the 1940s (Compo et al., 2011; Douville et al., 2017), the 20CR2 product is deemed probably unreliable for the early part of the record (Krueger et al., 2013). Therefore, we confined our analysis of the 20CR2 data to the period after 1940. The

surface heat fluxes (turbulent and radiative components) in the 20CR2 are calculated by the coupled model and thus should be interpreted with caution (Compo et al., 2011; O'Reilly & Zanna, 2018). Several previous studies have employed the heat flux data from 20CR2 reanalysis to investigate the thermodynamic processes associated with multidecadal SST variability (Gulev et al., 2013; Li et al., 2015; O'Reilly & Zanna, 2018; Sun et al., 2018), and the 20CR2 product has the ability to capture the observed SST-heat flux relationship. In particular, Gulev et al. (2013) showed that the correlations between North Atlantic decadal heat fluxes and SSTs derived from the 20CR2 reanalysis are qualitatively similar to the heat fluxes obtained only from ship observations. Area-weighted average of North Atlantic SST anomalies (0°–60°N, 80°W–0°) is used to define the AMO index (Zhang et al., 2016), and the Arabian Sea SST index is defined for the region (0°–30°N, 45°–75°E).

2.2. Statistical Methods

The long-term linear trends for the post-1900 period are removed by using the least squares method, and the aim is to better isolate and highlight the signal of decadal to multidecadal variability with the removal of the centennial-scale trends. In fact, removing a least squares quadratic fit of the secular warming trend (Enfield & Cid-Serrano, 2009) gives qualitatively similar results (see details in the supporting information). The data are low-pass filtered by applying an 11-year running mean in the analyses to focus on the multidecadal variability, and thus, the number of degrees of freedom is reduced. We access the statistical significance of the correlation coefficients using effective number of degrees of freedom and a two-tailed Student's t test (Li et al., 2013).

2.3. Model and Experiments

We use the general circulation model (GCM) developed by the International Centre of Theoretical Physics (ICTPAGCM, Version 41; Kucharski et al., 2016) to set up two experiments: Atlantic Pacemaker experiments with a slab ocean model (ATL_VARMIX) and the AGCM alone (ATL_VARAGCM). The introduction of GCM and the details about the experimental setup configuration of the ATL_VARMIX and ATL_VARAGCM simulations are given in the supporting information. An SST-forced-AGCM sensitivity experiment was carried out using the ICTPAGCM to investigate winter atmospheric circulation responses to the western Pacific (WP) SST forcing. The sensitivity and control runs were integrated for 12 and 15 years (longer than the sensitivity run to derive a steady reference state), respectively. The last 10 years of the integration are used to construct a 10-member ensemble to reduce the uncertainties due to different initial conditions. The WP SST forcing imposed in the sensitivity run was 5 times the WP regional SST anomaly regression on the AMO index (0°N–25°N, 130°E–170°E), and WP SST forced atmospheric responses are defined as the differences in the ensemble mean between the sensitivity and control runs with a scale factor of 1/5 (Sun et al., 2017; Sutton & Hodson, 2007). This scaling procedure enables to estimate the atmospheric response with shorter integrations. Another SST-forced-AGCM sensitivity experiment is similar but for the SST forcing with SST anomalies over the WP and North Atlantic prescribed simultaneously.

3. Results

3.1. Recent AS Warming Acceleration

To show the warming acceleration around the early 1990s, we calculate the difference in the warming trend between two periods of equal length, one during 1992–2013 and the other during 1970–1991. Over the AS (0–30°N, 45°E-75°E), there is indeed an increase of AS SST warming since the early 1990s (0.07 °C per decade and 0.13 °C per decade in the early and late periods, respectively), and this warming acceleration is most pronounced over the northern AS (Figure 1a). The increases of the SST warming trend are consistent throughout the three SST data sets (HadSST3, Kaplan, and ERSST products as indicated in section 2).

As shown in Figures 1b and S1, the increase of AS warming trend is the strongest in spring, followed by autumn and summer, while in winter the AS exhibits an SST warming slowdown around the early 1990s. In spring, the average increase of AS warming trend among the three SST data sets reaches 0.14 °C per decade, more than twice larger than that in summer and autumn. The spatial feature of the spring AS warming acceleration strongly projects onto the annual mean (Figures 1a and 1b); over the northern basin of the AS, the trend increase is particularly marked and consistent across the observational data sets.

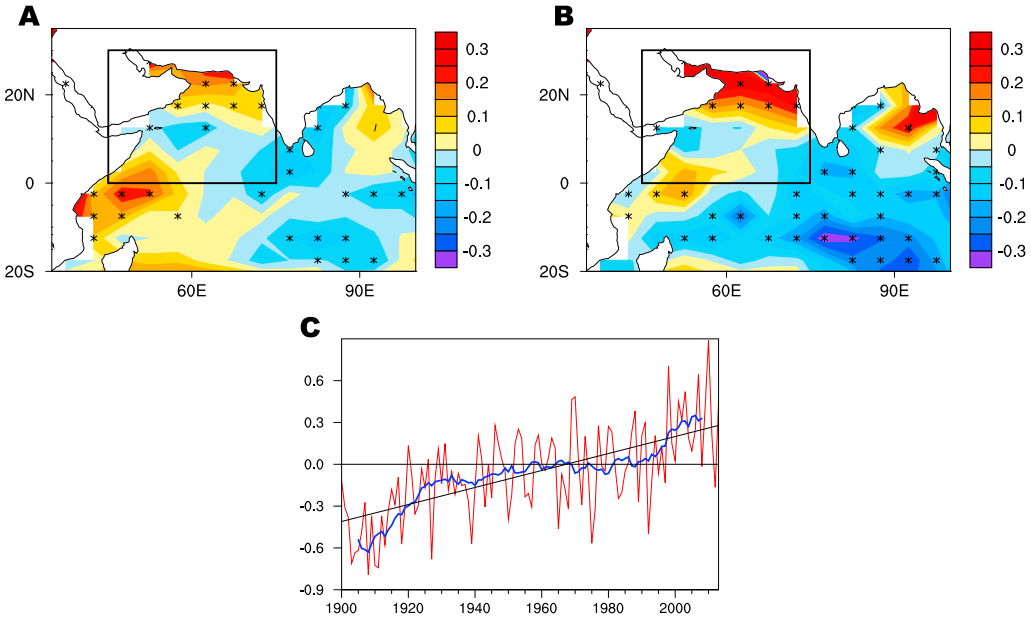

Figure 1. Main features of the recent acceleration of Arabian Sea warming since the 1990s. (a) Differences in annual SST linear trends (K per decade) between two equal-length periods after and before 1991 (1992–2013 and 1970–1991) over the Indian Ocean. (b) As in (a), but for the spring SST. In (a) and (b), the areas where all three SST products agree on the sign of the trend difference are marked by stars.(c) Time series of spring AS SST index (defined as the SST anomaly averaged over 0–30°N, 45–75°E) (red line), low-pass-filtered index (blue line), and the long-term linear trend (black line).

The rapid warming of AS spring SST since the early 1990s is closely linked with AS multidecadal variability. The time series of AS spring SST clearly exhibits multidecadal fluctuations superposed upon the century-scale warming trend (Figure 1c). In particular, AS SST turned from a flattening trend to a rapid warming trend around the early 1990s. The three SST products show similar multidecadal variability (Figure S2), which becomes more evident after removing the century-scale warming trend (Figure S3).

3.2. Linkage Between AS Spring SST Multidecadal Variability and the AMO

The possible connections between AS spring multidecadal SST variability and the dominant decadal modes in global SST (i.e., IPO/PDO and AMO) are further investigated. The correlation between AS SST and IPO/PDO at decadal timescales is weak and inconsistent in sign among different SST data sets (Table S1). A significant relationship between the AMO and AS SST is found (Table S2). A strong positive correlation is observed in spring and remains positive throughout the year, although it becomes modest during summer and autumn. In addition, the correlation with the AMO is consistent among different SST data sets and is independent of the low-pass filtering and the influence of El Niño-Southern Oscillation (Table S2).

Figure 2a shows the correlation map of the AS SST index (regional mean SST anomalies) with SST anomalies in the Northern Hemisphere based on the decadally filtered data. The correlations over the North Atlantic basin is characterized by a pattern with significant positive value that resembles the AMO. The decadally filtered time series of the spring AMO and AS SST shows a strong coherence, and the recent rapid warming of the AS can be well explained by the transition of the AMO phase from the cold phase to warm phase (Figure 2c). Furthermore, the positive correlation between the AMO and AS SST is not only coherent during spring but is also significant when the AMO leads by a season. The correlation map of the spring AS SST index with the preceding winter SST anomalies shows the typical AMO pattern over the North Atlantic (Figure 2b), and there is also a significant coherence between the time series of AS spring SST and preceding winter AMO at decadal timescales (Figure 2c).

The ATL_VARMIX experiment (Atlantic Pacemaker experiment: atmospheric model coupled to a slab ocean model over the Indo-Pacific, whereas monthly varying observational SSTs prescribed over the Atlantic) well reproduces the AS spring multidecadal variability and its linkage with the AMO. In the

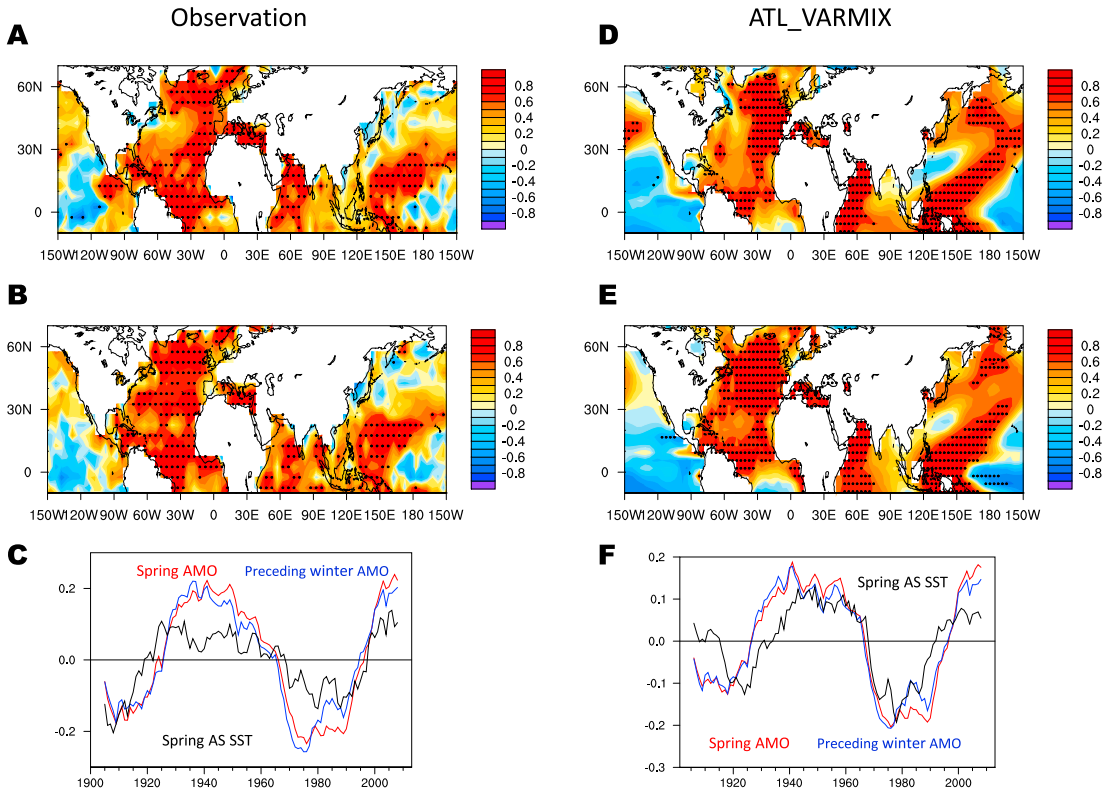

Figure 2. Observed and simulated connections between AS spring multidecadal SST variability and the AMO. (a) Correlation map between the spring AS SST index and the Northern Hemisphere SST based on decadally filtered data for the period 1900–2013 in the HadSST3 data set. (b) Correlation map between the spring AS SST index and preceding winter Northern Hemisphere SST at decadal timescales for the period 1900–2013. Dots in (a) and (b) indicate the correlations significant at the 95% confidence level. (c) Time series of low-pass-filtered indices of spring AS SST (black), spring AMO (red), and preceding winter AMO (blue) for the period 1900–2013. (d)–(f) As in (a)–(c), respectively, but for the simulation results from the ATL_VARMIX experiment.

simulation, the correlation map of the decadal AS SST index with the spring SST field (Figure 2d) is characterized by strong positive correlations across the North Atlantic, and this pattern also holds for the preceding winter SST field (Figure 2e), consistent with those observed (Figures 2a and 2b).

The simulated AS spring SST index also shows multidecadal variability, and the amplitude of this variability is comparable to the observation. The simulated AS multidecadal fluctuations are in good agreement with those observed (Figures 2c and 2f), also showing a rapid warming in recent decades. As expected, the correlations of the spring and preceding winter AMO with the simulated AS SST are high (Figure 2f).

Since the observed AS multidecadal variability and its connection with the AMO are well simulated by the ATL_VARMIX experiment in which the Indo-Pacific SST variation is solely driven by surface heat flux forcing, we perform a surface heat budget analysis to investigate the thermodynamic processes involved. We first examine the correlations of net surface heat flux anomalies during the preceding winter and spring seasons with the AS spring multidecadal variability using both reanalysis (20CR2) and ATL_VARMIX simulations.

Positive correlations are observed across the AS basin between the preceding winter surface heat flux and spring SST anomalies (Figure S4a). However, the relationship is almost reversed in spring, with the AS SST being negatively correlated with the contemporaneous spring heat flux anomalies over most of the AS basin (Figure S4b). The surface heat flux is defined to be positive downward, and thus, the opposite heat flux-SST relations indicate that the spring decadal SST anomalies are forced by the preceding winter surface heat flux anomalies while damped by the contemporaneous spring ones.

In the ATL_VARMIX experiment, the simulated heat flux-SST relation is consistent with the reanalysis (Figures S4c and S4d), and the forcing and damping effects of preceding winter and contemporaneous spring heat flux anomalies on the AS SST are respectively reproduced. Therefore, in both the reanalysis and slab-

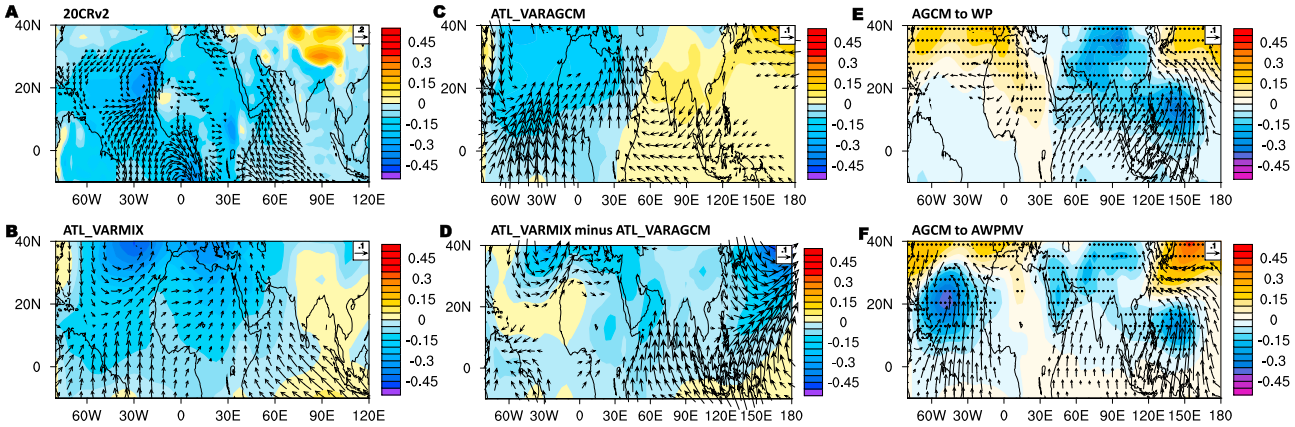

Figure 3. (a) Regression of SLP (hPa, shadings) and surface wind (m/s, vectors, omitted below 0.05 m/s) anomalies on the normalized AMO index at decadal timescales based on the 20CR2 reanalysis data. (b) As in (a), but for the SLP and surface wind data from the ATL_VARMIX simulation. (c) As in (b), but for the direct atmospheric responses to the AMO SST forcing in the ATL_VARAGCM simulations, shown as regressions onto the normalized AMO index at decadal timescales. (d) Effect of Indo-Pacific Ocean-atmosphere coupling, shown as the differences in the responses of SLP and winds to the AMO SST forcing between ATL_VARMIX and ATL_VARAGCM simulations. (e) Simulated atmospheric circulation responses of SLP and winds to warm SST anomalies over the WP region (0–25°N, 130–170°E) in the sensitivity experiments using the ICTPAGCM model. Dotted shading indicates the regions where the results from the sensitivity simulation are significantly different from the control simulation at the 95% confidence level (Student's *t* test). (f) As in (e), but for the responses to the warm SST anomalies over the Atlantic and WP prescribed simultaneously.

ocean-model simulation, the surface energy exchanges between the ocean and atmosphere during the preceding winter have an influential contribution to the SST tendency and play an essential forcing role in the onset and development of AS SST anomalies in the subsequent spring.

The different components of the forcing surface heat fluxes in the preceding winter are further analyzed in terms of their contribution to the net surface heat flux anomalies. The results from the reanalysis and ATL_VARMIX simulation are qualitatively consistent with each other (Figures S5 and S6), and we find that the turbulent fluxes (sensible plus latent heat fluxes) contribute most to the anomalous net surface heat flux and that the radiative components (longwave and shortwave radiative fluxes) seem to offset each other. In particular, the longwave radiation acts to play a forcing role in the SST variation, while the shortwave radiation plays a damping role. The opposing patterns of longwave and shortwave radiation anomalies may indicate a role of cloudiness, which has an opposite effect on the two radiative fluxes.

The surface heat flux anomalies are in close association with anomalous atmospheric conditions, and thus, the atmospheric circulation anomalies associated with the AMO during the preceding winter is analyzed to investigate the possible *atmospheric bridge* for the teleconnection to the AS basin. The regression pattern of sea level pressure (SLP) shows low anomalies over the North Atlantic and the AS basin (Figure 3a). The low SLP anomaly over the tropical North Atlantic is consistent with the SST forcing effect of the warm AMO phase. The anomalous low over the AS basin is accompanied by converging southerlies from the tropics.

Climatological northerlies are prevailing during the winter over the AS basin in association with the winter monsoon system (Figure S7). Therefore, the anomalous southerlies lead to a reduction of wind speed and a decrease in turbulent fluxes out of the ocean. This is consistent with the anomalous downward turbulent fluxes in the reanalysis (Figure S5). Meanwhile, the low-pressure anomalies over the AS correspond to anomalous ascending motion and increased convection and cloudiness (Figure S8), which can give rise to the decrease of surface longwave radiation loss and the reduction of incoming solar radiation (Figure S5).

The ATL_VARMIX simulated patterns of winter SLP and wind anomalies associated with the AMO warm phase resemble reanalysis and show an anomalous low and converging southerlies over the AS (Figure 3b), which in the slab ocean model lead to the positive anomalies of downward net surface heat flux (mostly from the turbulent fluxes) and warm SST tendency for the development of SST warming (Figure S6).

This pattern of winter atmospheric circulation anomalies and associated surface heat flux may also have an instantaneous warming effect on the AS ocean beneath, as implicated in the simultaneous positive correlation between the winter AMO and AS SST (Table S2). The warm AS SST anomaly in winter may reinforce

the anomalous low and converging southerlies due to its enhancing effect on local convective heating. Thus, the relationships between the wind reduction, anomalous downward turbulent heat flux, and SST warming over the AS suggest a positive wind-evaporation-SST feedback (Du & Xie, 2008; Xie & Philander, 1994), and this positive thermodynamic air-sea feedback can lead to an amplified SST warming, which persists to the subsequent spring, consistent with the positive correlations between the spring and preceding winter SST anomalies over the AS shown in Figure 2. The AS SST persistency from the preceding winter to spring is also seen in the unfiltered data from the observation and ATL_VARMIX simulation, independent of the low-pass filtering (Figure S9). Therefore, due to the profound impact on surface energy exchange, the atmospheric teleconnection pattern (the AS anomalous low and southerlies) associated with AMO SST warming in winter acts as a key atmospheric bridge for understanding the teleconnection from the AMO to the AS spring multidecadal variability.

3.3. The Role of Atlantic-Western Pacific Trans-basin Multidecadal Variability

A crucial issue is the generation of the anomalous low over the AS in response to the AMO SST warming: is it forced directly by the North Atlantic SST? To address this, we examine the simulation results from the ATL_VARAGCM experiment (atmospheric model forced directly by monthly varying observational SST prescribed over the Atlantic and climatological SST over the Indo-Pacific), which can reflect the atmospheric direct response to the Atlantic SST forcing of the AMO (Figure 3c). The ATL_VARAGCM simulates an anomalous low over the tropical North Atlantic, and this local atmospheric response to the AMO SST warming is similar to the ATL_VARMIX. However, there are remarkable differences in the remote atmospheric response over the Indian Ocean between the two experiments. In particular, over the AS basin, the anomalous low and converging southerlies simulated by the ATL_VARMIX are missing in the ATL_VARAGCM, and instead, high SLP anomalies and anomalous easterlies are simulated.

This atmospheric circulation pattern projects on an atmospheric Gill-type response to a north equatorial heating associated with North Atlantic SST warming (Gill, 1980; Li et al., 2016; Ruprich-Robert et al., 2017), and this warming produces equatorial Kelvin wave and Rossby wave to the eastern and western side of the heating source, respectively, which correspond to an east-west dipole pattern of SLP anomalies with an anomalous high and easterly wind anomalies over the Indian Ocean (Li et al., 2016). Although the Gill theory can explain the results from the ATL_VARAGCM experiment, it may not apply to the 20CR2 reanalysis and the ATL_VARMIX experiment (Figures 3a and 3b). The above two experiments differ only in the inclusion of atmosphere-ocean coupling outside the Atlantic basin, so the distinctive results may indicate that the atmosphere-ocean coupling in the Indo-Pacific basin plays the key role in the teleconnection between the AMO and the AS anomalous low.

The effects of the Indo-Pacific air-sea coupling on the atmospheric response to the AMO can be largely represented by the difference in the atmospheric circulation (e.g., SLP and surface winds) between ATL_VARMIX and ATL_VARAGCM experiments (ATL_VARMIX minus ATL_VARAGCM). As seen in Figure 3d, the remarkable differences in the tropical Indo-Pacific indeed suggest a strong effect of SST feedback on the atmospheric circulation response. Generally, anomalous low SLP and associated southerly cross-equatorial wind anomalies are seen across the northern Indian Ocean and WP. The SLP and surface wind anomalies over the WP are more pronounced than the Indian Ocean counterpart, possibly indicating a more important role of the air-sea coupling in the WP.

In fact, a recent study has suggested that there is a significant footprint of the AMO in the WP SST, producing an SST pattern of Atlantic-Western Pacific trans-basin multidecadal variability (AWPMV in short), which is formed through several processes including an atmospheric teleconnection from the North Atlantic to the North Pacific and feedbacks between the atmosphere and ocean in the subtropical and tropical Pacific (Sun et al., 2017). The AWPMV has also been identified as the leading mode of global internal decadal SST variability (Chen & Tung, 2018). Therefore, there emerges a reasonable hypothesis that the footprint of the AMO in the WP may establish the relationship between the AMO and the AS anomalous low in winter and the AWPMV plays the essential forcing role in AS multidecadal variability. The maps of Northern Hemisphere SST correlations with the AS multidecadal variability (Figure 2) provide statistical evidences for this hypothesis that there are high and significant correlations over the WP region, while over the eastern tropical Pacific the correlations are weak and negligible.

Two sensitivity experiments using the ICTPAGCM isolating the effects of the WP SST footprint of the AMO and the AWPMV were carried out to verify the above hypothesis (see section 2.3). First, we examine the SST anomaly pattern of AWPMV in winter for the bottom boundary conditions prescribed in the AGCM sensitivity experiments (Figure S10). Strong warm SST anomalies are observed over the North Atlantic and western Pacific basins associated with the AWPMV warm phase. In addition, positive SST anomalies are also seen in the northern Indian Ocean, indicating that the winter local atmospheric circulation anomalies (the anomalous low and southerlies) and associated net downward surface heat flux may have an instantaneous warming effect on the ocean beneath.

We further investigate the possible origin of the anomalous low and southerlies by analyzing the results from the sensitivity experiments. Forced by the WP SST anomalies alone (the WP box: 0–25°N, 130°E–170°E, shown in Figure S10), the AGCM simulation shows strong low-pressure anomalies and anomalous southerly cross-equatorial flow across the northern Indian Ocean and WP (Figure 3e), and the main features of the atmospheric circulation anomalies are in good agreement with the ATL_VARMIX minus ATL_VARAGCM response (Figure 3d). This pattern of atmospheric responses to the WP SST warming is also consistent with Gill's theory, which predicts that a north equatorial heating anomaly induces a response of low pressure at surface most pronounced to the northwest of the heating source (Figure 3e), corresponding to a stationary Rossby wave (Gill, 1980; Sutton & Hodson, 2007). The WP SST warming-induced Gill-type Rossby wave response, the low-pressure anomalies over the northern Indian Ocean and southern Asia (to the northwest of the WP), gives rise to strong cross-equatorial SLP gradient and thus leads to anomalous southerly cross-equatorial flow converging toward the northern Indian Ocean (Figures 3b and 3d).

The AGCM simulation forced by both the North Atlantic and WP SST anomalies of the AWPMV is further examined. The winter atmospheric circulation response to the AWPMV SST warming (simultaneous warming over the North Atlantic and WP) shows low-pressure anomalies over the tropical North Atlantic and WP, due to the local effect of SST forcing. Over the northern Indian Ocean and the AS basin, an anomalous low is simulated associated with converging southerlies from the tropics. It is noted that this anomalous low is slightly weaker than the AGCM simulation forced by the WP SST alone, possibly due to a suppressing effect of the equatorial Kelvin wave response induced by North Atlantic SST warming (Figure 3f).

Generally, the main features of the AGCM simulated response to the AWPMV SST forcing, that is, the low-pressure anomalies over both the tropical North Atlantic and AS, are consistent with the atmospheric teleconnection pattern associated with the AMO in the 20CR2 reanalysis and ATL_VARMIX experiment (Figures 3a and 3b). Following the formation of the anomalous low and southerly anomalies in winter, the positive wind-evaporation-SST feedback further develops, leading to strong warm SST tendency and significant spring SST warming over the AS. Therefore, the above two sensitivity experiments highlight the key role of the WP SST footprint of the AMO (i.e., SST anomalies of the AWPMV over the WP) in establishing the teleconnection from the AMO to AS multidecadal variability.

4. Conclusion

The rapid warming of the AS brings an increased risk of extreme weather and climate events such as floods, heat waves, and cyclones. Observational analysis suggests that the warming rate of the AS has significantly increased during the past two decades, mostly in the spring season, and this acceleration of AS warming is closely linked with multidecadal variability of AS spring SST. This variability is found unlikely to be explained by the Interdecadal Pacific Oscillation but closely related to the AMO.

A set of Atlantic pacemaker experiments with a slab mixed-layer ocean model successfully reproduces the AS spring multidecadal variability and its connection with the AMO, and an atmospheric teleconnection to the AS in the preceding winter and associated thermodynamic air-sea feedback are both found to be important. The atmospheric circulation model can simulate the teleconnection pattern when the AMO SST and its trans-basin footprint over the WP are prescribed simultaneously. The WP SST warming associated with the AMO positive phase induces a Gill-type Rossby wave response over the AS, showing an anomalous low and converging southerlies that weaken the winter monsoon northerlies. A positive wind-evaporation-SST feedback further develops, leading to an amplified AS SST warming, which persists to the subsequent spring. Therefore, the concurrent cold-to-warm phase shift of the AMO and its WP SST footprint since the 1990s contributes constructively to the recent acceleration of AS warming.

The positive radiative forcing associated with the increased atmospheric greenhouse gas concentrations gives rise to the century-scale warming trend of the Indian Ocean SST. Even though, the multidecadal warming rate of Indian Ocean SST varies from time to time and in different areas, and this may be partly due to the natural external radiative forcing, such as volcanic aerosols and solar irradiance changes (Dong & McPhaden, 2017a). However, the basin-wide SSTs may share a synchronous variation under the external forcing (Dong & McPhaden, 2017a), and the recent AS warming acceleration and its different features from other parts of the Indian Ocean (Figure 1) are unlikely to be solely explained by the effect of external forcing, suggesting a role of internal climate variability.

We have identified the AMO and its trans-basin SST footprint over the WP as a major factor contributing to AS multidecadal variability and the recent rapid warming. As the AMO shows long persistence of phase and relatively high decadal predictability, which mainly stems from the Atlantic Meridional Overturning Circulation (Keenlyside et al., 2008; Trenary & DelSole, 2016; Yan et al., 2018). This can be applied to the predictions of future episodes of the AS warming acceleration and slowdown. This has important implications given that the climate and the hydrological cycle over the surrounding regions are sensitive to the thermal state of the AS basin.

Acknowledgments
The original observational and atmospheric reanalysis data sets are publicly available from the corresponding websites (ERSST, Kaplan, HadSST3, and 20CRv2, at https://www.esrl.noaa.gov/psd/data/gridded/data.noaa.ersst.v3.html, https://www.esrl.noaa.gov/psd/data/gridded/data.kaplan_sst.html, http://www.metoffice.gov.uk/hadobs/hadsst3/, and https://www.esrl.noaa.gov/psd/data/gridded/). The model output used in the figures for the experiments of this study is available at Zenodo (https://doi.org/10.5281/zenodo.1476823). The authors wish to thank the three anonymous reviewers for their constructive comments that significantly improved the quality of this paper. This work was jointly supported by the National Natural Science Foundation of China (41731173), the National Programme on Global Change and Air-Sea Interaction (GASI-IPOVAI-03&GASI-IPOVAI-06), and the National Key R&D Program of China (2016YFA0601801). C.S. is supported by the State Key Laboratory of Tropical Oceanography, South China Sea Institute of Oceanology, Chinese Academy of Sciences (Project LTO1801). C.W. is supported by the Pioneer Hundred Talents Program of the Chinese Academy of Sciences and the Leading Talents of Guangdong Province Program.

References

Chen, X. Y., & Tung, K. K. (2018). Global-mean surface temperature variability: Space-time perspective from rotated EOFs. *Climate Dynamics*, *51*(5–6), 1719–1732. https://doi.org/10.1007/s00382-017-3979-0

Compo, G. P., Whitaker, J. S., Sardeshmukh, P. D., Matsui, N., Allan, R. J., Yin, X., et al. (2011). The twentieth century reanalysis project. *Quarterly Journal of the Royal Meteorological Society*, *137*(654), 1–28. https://doi.org/10.1002/qj.776

Deser, C., Phillips, A. S., & Hurrell, J. W. (2004). Pacific interdecadal climate variability: Linkages between the tropics and the North Pacific during boreal winter since 1900. *Journal of Climate*, *17*(16), 3109–3124. https://doi.org/10.1175/1520-0442(2004)017<3109:PICVLB>2.0.CO;2

Dinesh Kumar, P. K., Paul, Y. S., Muraleedharan, K. R., Murty, V. S. N., & Preenu, P. N. (2016). Comparison of long-term variability of sea surface temperature in the Arabian Sea and Bay of Bengal. *Regional Studies in Marine Science*, *3*, 67–75. https://doi.org/10.1016/j.rsma.2015.05.004

D'Mello, J. R., & Prasanna Kumar, S. (2018). Processes controlling the accelerated warming of the Arabian Sea. *International Journal of Climatology*, *38*(2), 1074–1086. https://doi.org/10.1002/joc.5198

Dong, L., & McPhaden, M. J. (2017a). The role of external forcing and internal variability in regulating global mean surface temperatures on decadal timescales. *Environmental Research Letters*, *12*(3). https://doi.org/10.1088/1748-9326/aa5dd8

Dong, L., & Mcphaden, M. J. (2017b). Why has the relationship between Indian and Pacific Ocean decadal variability changed in recent decades? *Journal of Climate*, *30*(6), 1971–1983. https://doi.org/10.1175/JCLI-D-16-0313.1

Dong, L., Zhou, T. J., Dai, A. G., Song, F. F., Wu, B., & Chen, X. L. (2016). The footprint of the inter-decadal Pacific oscillation in Indian Ocean Sea surface temperatures. *Scientific Reports*, *6*.

Douville, H., Peings, Y., & Saint-Martin, D. (2017). Snow-(N)AO relationship revisited over the whole twentieth century. *Geophysical Research Letters*, *44*, 569–577. https://doi.org/10.1002/2016GL071584

Du, Y., & Xie, S.-P. (2008). Role of atmospheric adjustments in the tropical Indian Ocean warming during the 20th century in climate models. *Geophysical Research Letters*, *35*, L08712. https://doi.org/10.1029/2008GL033631

Enfield, D. B., & Cid-Serrano, L. (2009). Secular and multidecadal warmings in the North Atlantic and their relationships with major hurricane activity. *International Journal of Climatology*. https://doi.org/10.1002/joc.1881

Enfield, D. B., Mestas-Nunez, A. M., & Trimble, P. J. (2001). The Atlantic multidecadal oscillation and its relation to rainfall and river flows in the continental US. *Geophysical Research Letters*, *28*(10), 2077–2080. https://doi.org/10.1029/2000GL012745

Folland, C. K., Rayner, N. A., Brown, S. J., Smith, T. M., Shen, S. S. P., Parker, D. E., et al. (2001). Global temperature change and its uncertainties since 1861. *Geophysical Research Letters*, *28*(13), 2621–2624. https://doi.org/10.1029/2001GL012877

Gill, A. E. (1980). Some simple solutions for heat-induced tropical circulation. *Quarterly Journal of the Royal Meteorological Society*, *106*(449), 447–462. https://doi.org/10.1002/qj.49710644905

Gulev, S. K., Latif, M., Keenlyside, N., Park, W., & Koltermann, K. P. (2013). North Atlantic Ocean control on surface heat flux on multi-decadal timescales. *Nature*, *499*(7459), 464–467. https://doi.org/10.1038/nature12268

Han, W. Q., Meehl, G. A., Hu, A. X., Alexander, M. A., Yamagata, T., Yuan, D. L., et al. (2014). Intensification of decadal and multi-decadal sea level variability in the western tropical Pacific during recent decades. *Climate Dynamics*, *43*(5–6), 1357–1379. https://doi.org/10.1007/s00382-013-1951-1

Han, W. Q., Vialard, J., McPhaden, M. J., Lee, T., Masumoto, Y., Feng, M., & De Ruijter, W. P. M. (2014). Indian Ocean decadal variability: A review. *Bulletin of the American Meteorological Society*, *95*(11), 1679–1703.

Izumo, T., Montégut, C. B., Luo, J.-J., Behera, S. K., Masson, S., & Yamagata, T. (2008). The role of the western Arabian Sea upwelling in Indian monsoon rainfall variability. *Journal of Climate*, *21*(21), 5603–5623. https://doi.org/10.1175/2008JCLI2158.1

Kaplan, A., Cane, M. A., Kushnir, Y., Clement, A. C., Blumenthal, M. B., & Rajagopalan, B. (1998). Analyses of global sea surface temperature 1856-1991. *Journal of Geophysical Research*, *103*(C9), 18,567–18,589. https://doi.org/10.1029/97JC01736

Keenlyside, N. S., Latif, M., Jungclaus, J., Kornblueh, L., & Roeckner, E. (2008). Advancing decadal-scale climate prediction in the North Atlantic sector. *Nature*, *453*(7191), 84–88. https://doi.org/10.1038/nature06921

Kennedy, J. J., Rayner, N. A., Smith, R. O., Parker, D. E., & Saunby, M. (2011). Reassessing biases and other uncertainties in sea surface temperature observations measured in situ since 1850: 1. Measurement and sampling uncertainties. *Journal of Geophysical Research*, *116*, D14103. https://doi.org/10.11029/12010JD015218

Knight, J. R., Allan, R. J., Folland, C. K., Vellinga, M., & Mann, M. E. (2005). A signature of persistent natural thermohaline circulation cycles in observed climate. *Geophysical Research Letters*, *32*, L20708. https://doi.org/10.1029/2005GL024233

Krueger, O., Schenk, F., Feser, F., & Weisse, R. (2013). Inconsistencies between long-term trends in storminess derived from the 20CR reanalysis and observations. *Journal of Climate*, *26*(3), 868–874. https://doi.org/10.1175/JCLI-D-12-00309.1

Kucharski, F., Ikram, F., Molteni, F., Farneti, R., Kang, I.-S., No, H.-H., et al. (2015). Atlantic forcing of Pacific decadal variability. *Climate Dynamics*, *46*(7–8), 2337–2351.

Kucharski, F., Parvin, A., Rodriguez-Fonseca, B., Farneti, R., Martin-Rey, M., Polo, I., et al. (2016). The teleconnection of the tropical Atlantic to Indo-Pacific sea surface temperatures on inter-annual to centennial time scales: A review of recent findings. *Atmosphere*, *7*(2), 29. https://doi.org/10.3390/atmos7020029

Kumar, S. P., Roshin, R. P., Narvekar, J., Kumar, P. K., & Vivekanandan, E. (2009). Response of the Arabian Sea to global warming and associated regional climate shift. *Marine Environment Research*, *68*(5), 217–222. https://doi.org/10.1016/j.marenvres.2009.06.010

Li, J. P., Sun, C., & Jin, F. F. (2013). NAO implicated as a predictor of Northern Hemisphere mean temperature multidecadal variability. *Geophysical Research Letters*, *40*, 5497–5502. https://doi.org/10.1002/2013GL057877

Li, T., Zhang, Y., Chang, C. P., & Wang, B. (2001). On the relationship between Indian Ocean sea surface temperature and Asian summer monsoon. *Geophysical Research Letters*, *28*(14), 2843–2846. https://doi.org/10.1029/2000GL011847

Li, X. C., Xie, S. P., Gille, S. T., & Yoo, C. (2016). Atlantic-induced pan-tropical climate change over the past three decades. *Nature Climate Change*, *6*(3), 275–279. https://doi.org/10.1038/nclimate2840

Li, Y., Li, J. P., Zhang, W. J., Zhao, X., Xie, F., & Zheng, F. (2015). Ocean dynamical processes associated with the tropical Pacific cold tongue mode. *Journal of Geophysical Research: Oceans*, *120*, 6419–6435. https://doi.org/10.1002/2015JC010814

Lovsletten, O., & Rypdal, M. (2016). Statistics of regional surface temperatures after 1900: Long-range versus short-range dependence and significance of warming trends. *Journal of Climate*, *29*(11), 4057–4068. https://doi.org/10.1175/JCLI-D-15-0437.1

Murakami, H., Vecchi, G. A., & Underwood, S. (2017). Increasing frequency of extremely severe cyclonic storms over the Arabian Sea. *Nature Climate Change*, *7*(12), 885–889. https://doi.org/10.1038/s41558-017-0008-6

O'Reilly, C. H., & Zanna, L. (2018). The signature of oceanic processes in decadal extratropical SST anomalies. *Geophysical Research Letters*, *45*, 7719–7730. https://doi.org/10.1029/2018GL079077

Parker, D., Folland, C., Scaife, A., Knight, J., Colman, A., Baines, P., & Dong, B. W. (2007). Decadal to multidecadal variability and the climate change background. *Journal of Geophysical Research*, *112*, D18115. https://doi.org/10.1029/2007JD008411

Roxy, M. K., Ghosh, S., Pathak, A., Athulya, R., Mujumdar, M., Murtugudde, R., et al. (2017). A threefold rise in widespread extreme rain events over central India. *Nature Communications*, *8*(1). https://doi.org/10.1038/s41467-017-00744-9

Roxy, M. K., Ritika, K., Terray, P., & Masson, S. (2014). The curious case of Indian Ocean warming. *Journal of Climate*, *27*(22), 8501–8509. https://doi.org/10.1175/JCLI-D-14-00471.1

Roxy, M. K., Ritika, K., Terray, P., Murtugudde, R., Ashok, K., & Goswami, B. N. (2015). Drying of Indian subcontinent by rapid Indian Ocean warming and a weakening land-sea thermal gradient. *Nature Communications*, *6*(1). https://doi.org/10.1038/ncomms8423

Ruprich-Robert, Y., Msadek, R., Castruccio, F., Yeager, S., Delworth, T., & Danabasoglu, G. (2017). Assessing the climate impacts of the observed Atlantic multidecadal variability using the GFDL CM2.1 and NCAR CESM1 global coupled models. *Journal of Climate*, *30*(8), 2785–2810. https://doi.org/10.1175/JCLI-D-16-0127.1

Schott, F. A., Xie, S.-P., & McCreary, J. P. (2009). Indian Ocean circulation and climate variability. *Reviews of Geophysics*, *47*, RG1002. https://doi.org/10.1029/2007RG000245

Shukla, J., & Misra, B. M. (1977). Relationships between sea-surface temperature and wind speed over central Arabian Sea, and monsoon rainfall over India. *Monthly Weather Review*, *105*(8), 998–1002. https://doi.org/10.1175/1520-0493(1977)105<0998:RBSSTA>2.0.CO;2

Smith, T. M., Reynolds, R. W., Peterson, T. C., & Lawrimore, J. (2008). Improvements to NOAA's historical merged land-ocean surface temperature analysis (1880-2006). *Journal of Climate*, *21*(10), 2283–2296. https://doi.org/10.1175/2007JCLI2100.1

Sun, C., Kucharski, F., Li, J. P., Jin, F. F., Kang, I. S., & Ding, R. Q. (2017). Western tropical Pacific multidecadal variability forced by the Atlantic multidecadal oscillation. *Nature Communications*, *8*. https://doi.org/10.1038/ncomms15998

Sun, C., Li, J., & Jin, F.-F. (2015). A delayed oscillator model for the quasi-periodic multidecadal variability of the NAO. *Climate Dynamics*, 1–17.

Sun, C., Li, J. P., Li, X., Xue, J. Q., Ding, R. Q., Xie, F., & Li, Y. (2018). Oceanic forcing of the interhemispheric SST dipole associated with the Atlantic Multidecadal Oscillation. *Environmental Research Letters*, *13*(7). https://doi.org/10.1088/1748-9326/aacf66

Sutton, R. T., & Hodson, D. L. R. (2007). Climate response to basin-scale warming and cooling of the North Atlantic Ocean. *Journal of Climate*, *20*(5), 891–907. https://doi.org/10.1175/JCLI4038.1

Swanson, K. L., Sugihara, G., & Tsonis, A. A. (2009). Long-term natural variability and 20th century climate change. *Proceedings of the National Academy of Sciences of the United States of America*, *106*(38), 16,120–16,123. https://doi.org/10.1073/pnas.0908699106

Trenary, L., & DelSole, T. (2016). Does the Atlantic Multidecadal Oscillation get its predictability from the Atlantic Meridional Overturning Circulation? *Journal of Climate*, *29*(14), 5267–5280. https://doi.org/10.1175/JCLI-D-16-0030.1

Trenberth, K. E., Jones, P. D., Ambenhe, P., Bojariu, R., Easterling, D., Tank, A. K., et al. (2007). Observations: Surface and atmospheric climate change. In S. Solomon (Ed.), *Climate change 2007: The physical science basis* (pp. 747–845). Cambridge, UK: Cambridge Univ Press.

Trenberth, K. E., & Fasullo, J. T. (2012). Climate extremes and climate change: The Russian heat wave and other climate extremes of 2010. *Journal of Geophysical Research-Atmospheres*, *117*, D17103. https://doi.org/10.1029/2012JD018020

Vecchi, G. A., Xie, S. P., & Fischer, A. S. (2004). Ocean-atmosphere covariability in the western Arabian Sea. *Journal of Climate*, *17*(6), 1213–1224. https://doi.org/10.1175/1520-0442(2004)017<1213:OCITWA>2.0.CO;2

Vinayachandran, P. N. (2004). Summer cooling of the Arabian Sea during contrasting monsoons. *Geophysical Research Letters*, *31*, L13306. https://doi.org/10.1029/2004GL019961

Xie, S. P., & Philander, S. G. H. (1994). A coupled ocean-atmosphere model of relevance to the ITCZ in the eastern Pacific. *Tellus Series A-Dynamic Meteorology andOceanography*, *46*(4), 340–350.

Yan, X. Q., Zhang, R., & Knutson, T. R. (2018). Underestimated AMOC variability and implications for AMV and predictability in CMIP models. *Geophysical Research Letters*, *45*, 4319–4328. https://doi.org/10.1029/2018GL077378

Zhang, R., & Delworth, T. L. (2007). Impact of the Atlantic Multidecadal Oscillation on North Pacific climate variability. *Geophysical Research Letters*, *34*, L23708. https://doi.org/10.21029/22007GL031601

Zhang, R., Sutton, R., Danabasoglu, G., Delworth, T. L., Kim, W. M., Robson, J., & Yeager, S. G. (2016). Comment on "The Atlantic Multidecadal Oscillation without a role for ocean circulation". *Science*, *352*(6293), 1527. https://doi.org/10.1126/science.aaf1660